

Received November 28, 2019, accepted December 11, 2019, date of publication December 16, 2019, date of current version December 27, 2019.

Digital Object Identifier 10.1109/ACCESS.2019.2959812

Integrated VONE Scheme Over Resource-Virtualized Elastic Optical Networks

MIN ZHU^{1,2}, TIANYU SHEN³, QING SUN⁴, BIN CHEN³, AND JIAHUA GU¹

¹National Mobile Communications Research Laboratory, Southeast University, Nanjing 210096, China

²Purple Mountain Laboratories, Nanjing 211111, China

³School of Electronic Science and Engineering, Southeast University, Nanjing 210096, China

⁴Huawei Technology Company, Ltd., Nanjing 210012, China

Corresponding author: Min Zhu (minzhu@seu.edu.cn)

This work was supported by the National Natural Science Foundation of China (NSFC) under Grant 61771134.

ABSTRACT To eliminate the ossification of optical infrastructure and adapt to the high-performance Internet applications, optical network virtualization is an important enabler to offer each application type a dedicated virtual optical network (VON). It can provide resource sharing for multiple VON requests on an optical infrastructure, and promise efficient use of network resources. In the paper, we first introduce a new concept of resource-virtualized elastic optical network (RvEON), which not only realizes link-tier spectrum virtualization in each substrate fiber link (SFL), but also node-tier virtualized transponders (vTPs) within each substrate node (SN). The RvEON can be considered as a very promising optical infrastructure for multiple VON requests. We then propose a novel integrated virtual optical network embedding (iVONE) scheme over RvEONs. For the iVONE, the node mapping and link mapping are performed in an integrated way, which is totally different from all existing two-phased VONE schemes. In the RvEONs, a novel integer linear programming (ILP) model is formulated, which additionally takes into account the subcarrier and modulator resource constraints of the virtualized TPs. Meanwhile, a novel routing, modulator, spectrum and subcarrier assignment (RMS²A) algorithm is designed to establish lightpaths for virtual link mapping in the RvEONs. The simulation results demonstrate that our proposed RMS²A algorithm achieves better performance than the existing benchmark two-phased algorithm. We also investigate the impact of bit-rates of the VON requests and the different configurations of various modulators that each vTP can offer on the network performances, respectively.

INDEX TERMS Elastic optical networks, network resource virtualization, virtual optical network embedding, virtualized transponder.

I. INTRODUCTION

Recently, Internet applications such as big data and cloud computing are emerging. These applications usually have their own resource usage and network access pattern, which requires dedicated network services that can provide specific bit-rate and quality of service (QoS) (e.g., transmission delay) [1]. To address these issues, optical network virtualization has been considered as a promising technology to promote the development of the next-generation Internet applications [2]–[3]. Specifically, it can provision dedicated virtual optical network (VON) slice to serve different applications with specific QoS requirements. In particular, a VON request can be constructed for each specific

application and multiple VONs share same physical infrastructure including both the link and node resources in entire substrate network [4]. A VON request is composed of several virtual nodes (VNs) interconnected by virtual optical links (VOLs). Typically, the process of allocating the physical substrate network's resources to the VON requests is called as virtual optical network embedding (VONE). During this VONE, each VN is mapped to a substrate node (SN), and each VOL is mapped to a lightpath including one or more substrate fiber links (SFLs) in the physical network.

As we know, the VONE can be classified into offline (or static) and online (or dynamic) problems depending on different network scenarios [5]. The offline VONE problems, corresponding to the static network scenario, address the schemes where all the VON requests are known in advance and their occupied resources will never be released. In online

The associate editor coordinating the review of this manuscript and approving it for publication was Qunbi Zhuge.

network scenario, each VON request, which has an arrival time and lifetime, can come in and depart dynamically and is not known before its arrivals. Also, these VON requests can be provisioned or terminated at any moment dynamically. The resources previously utilized by the terminated requests need to be released in time when its lifetime is over and reallocated to new arrival requests.

With respect to the substrate networks, the introduction of elastic optical networking (EON) [6] with flexible grids has been proposed as a promising technology recently. It allows the optical spectra of fiber link to be flexibly segmented and aggregated at the granularity of a few gigahertz (e.g. 12.5 GHz), which, in a sense, realizes *link-tier optical spectra virtualization*. Meanwhile, virtualizable bandwidth variable transponder (V-BVT) has been proposed too. It is the *node-tier optical transponder virtualization*. In [7], a novel V-BVT architecture was presented and both online and offline virtualization algorithms for V-BVT were introduced. In [8], another feasible V-BVT architecture was presented by provisioning an optical subcarrier pool and an optical modulator pool within each SN. The former consists of one or multiple multi-wavelength source lasers, which generates a group of optical subcarriers. The latter contains a set of different local optical modulators, offering myriad modulation formats. A specific virtualization algorithm for V-BVT was also proposed to create multiple virtualized transponders (vTPs) (i.e., vTP slices). Each created vTP can offer flexible bandwidth with independent modulation format and baud rate to establish elastic lightpaths, based on each VON's QoS requirements. These lightpaths possibly originated from same one physical TP can target different destinations. Hence, the realization of the vTPs can greatly increase the TP resource utilization and improve the network traffic transmission efficiency. Based on these existing works, we introduced a novel concept of resource-virtualized EON (RvEON), which can realize both the link-tier spectrum virtualization and the node-tier TP virtualization.

Some studies have investigated the VONE over traditional fixed-grid wavelength division multiplexing (WDM) networks. A mixed integer linear programming (ILP) model was formulated and two greedy heuristic were proposed for offline VONE in WDM networks in [9]. In [10], by considering physical layer impairments (PLIs), algorithms were designed to achieve online PLI-aware VONE in WDM networks. In [11], focusing on link mapping, several ILP models were formulated for VONE in WDM networks.

Recently, several studies have suggested that the VONE over flexible-grid EONs can be more flexible and efficient. Lin *et al.* [12] considered the VONE problem with dynamic traffic in flex-grid networks. Although different modulation modes were used in optical channels to reduce the spectrum usage, they ignored the resources of subcarriers within the vTPs. In [13], the link mapping was considered in EONs, but node mapping was not addressed. In [14], a simple ILP model that only consider one single VON request was formulated in EONs, and two heuristic algorithms were

proposed, where the node mapping and link mapping are performed separately. In [15], authors also performed the node mapping and link mapping separately when considering VONE in elastic optical inter-DC networks. For node mapping, betweenness was introduced to measure the importance of a substrate node. For link mapping, fragmentation status of the link was considered to arrange the spectral in a more compact way to improve the spectral efficiency. In [16], the risk-aware VNE (RVNE) problem was investigated in optical data center networks. A novel RVNE heuristic algorithm performing the physical isolation between risky and safe virtual machines (VMs) was proposed to guarantee the security of the system. Nguyen *et al.* [17] introduced a real-time VNE strategy to maximize the economic benefit by defining a function of the long-term average revenue. In [18], the authors proved the NP-Completeness of the VONE over EONs and proposed two mathematical models. In [19], a generic preprocessing mechanism called NeuroViNE was proposed. By extracting subgraphs from the substrate network, this approach can either improve runtime or embedding quality of the existing VNE algorithms.

However, in all existing works, there are two noteworthy issues. First, the virtualized resource provisioning of subcarrier and modulator resources within the TPs are not considered in all existing VONE. In other words, only the spectrum resources of the SFLs are assigned for the VON requests, but *the TP resources of the SN are ignored*. Second and more importantly, in these existing VONE schemes, all the VNs are mapped in the first phase, while the VOL mapping is performed in the second phase. The two mapping procedures are independent of each other. Specifically, *the "two-phased VONE scheme" overlooks the mutual influence between the two mapping procedures, which incurs larger VON request blocking* (see simulation results of this paper).

In this paper, our contributions can be summarized as follows. 1) To the best of our knowledge, we are the first to propose *a novel integrated VONE (iVONE) scheme*, where the node mapping and link mapping are performed in an integrated way. 2) We will view the RvEON as the substrate networks. Thus, during the proposed iVONE, it requires *coordinated utilization of all virtualized substrate resources*, including the spectrum slot resources in each SFL, the subcarrier and modulator resources of the virtualized TPs in each SN. Hence, it is a new challenge to embed multiple VONs in the RvEONs in a cost-effective way. 3) An ILP model for VONE scheme that involves the vTP resource allocation is formulated to obtain the optimal solution. 4) Due to the non-scalability of the ILP model, we design offline and online heuristic iVONE algorithms. In these heuristic algorithms, we develop a virtual-auxiliary-graph (VAG) approach, where the subcarriers within the vTPs are treated the same as the frequency slots (FSs) of the SFLs. As a result, the substrate RvEON is decomposed into several layered graphs, according to the bit-rate requirement of a VON request. In each VAG sub-layer, we design a novel routing, modulation, spectrum and subcarrier assignment (RMS²A)

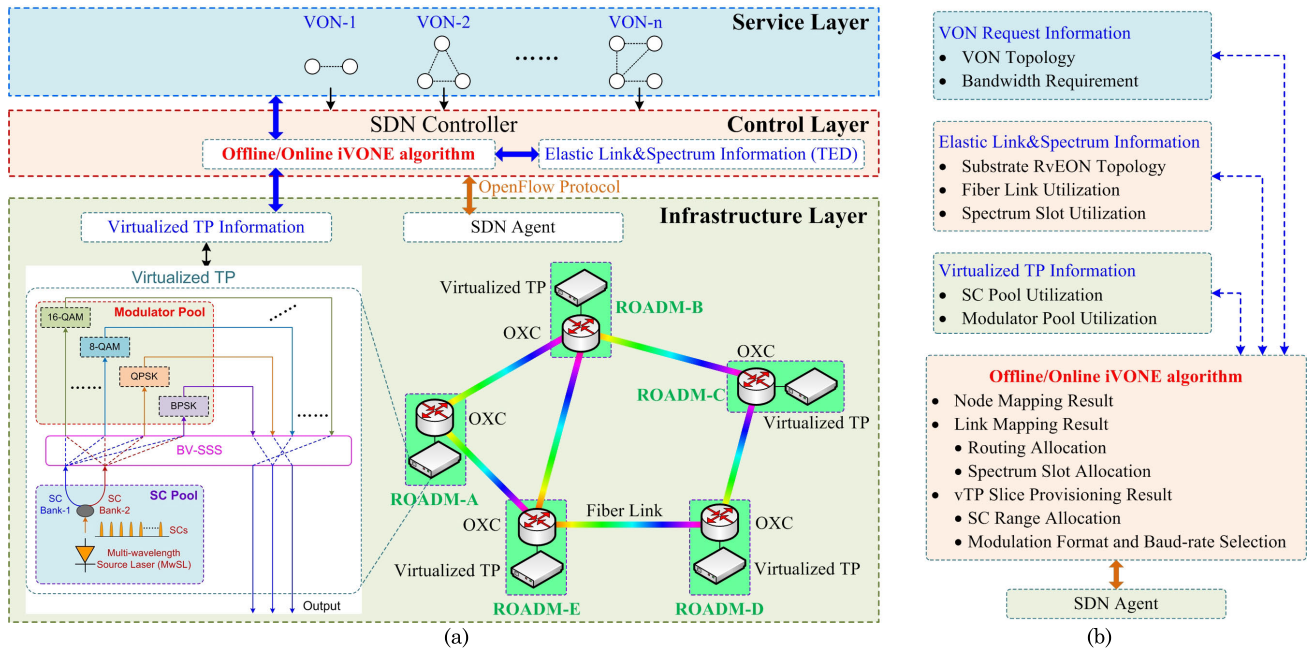


FIGURE 1. (a) RvEON architecture with virtualized TPs, and (b) Relationships between the main control module “offline/online iVONE algorithm” and other function modules.

algorithm to setup elastic lightpaths for all VOLs, with the consideration of the transmission reach (TR) constraint of available modulators.

The rest of this paper is organized as follows. Section II introduces the concept and architecture of the RvEONs. The RvEON model and the transparent VONE problem are described in section III, with the consideration of the TP virtualization within SNs. In section IV, a novel ILP model is formulated with the consideration of the vTP resources. The iVONE offline and online heuristic algorithms are designed in section V, including the VAG method and RMS²A heuristics. Extensive simulation results are given out in section VI. We finally summarize the paper in Section VII.

II. CONCEPT AND ARCHITECTURE OF RVEON

For clarity, we introduce in this section a new concept of RvEON, which can realize both the link-tier spectrum virtualization and the node-tier TP virtualization. In Fig. 1, we provide a high-level overview on the RvEON architecture based on some existing architectures [6]–[7], and then explain the designs of the three layers in the architecture in details.

With software defined networking (SDN), we aim to integrate the virtualized-TPs into spectrum-virtualized EON to achieve on-demand VON slicing over multi-dimensional resource-virtualized EONs. Here, a VON slice contains not only guaranteed spectrum resources of the SFLs in the form of VOLs, but also coexisting and isolated vTPs in the form of VNs. Note that, these resources assigned for a VON slice are related to each other. Specifically, in a transparent VON, the subcarriers of the vTPs assigned for VNs occupy the same optical spectrum range as that of the frequency slots (FSs) assigned for VOLs. Moreover, for a given VON bandwidth

requirement, adaptive modulators of the vTPs assigned for VNs also determine how many FSs are used for the VOLs. Therefore, during the proposed iVONE, it requires *coordinated utilization of all virtualized substrate resources in the RvEON*. Figure 1(a) shows the architecture of the RvEON, where there are three layers in it as follows.

A. INFRASTRUCTURE LAYER

This layer is the substrate optical infrastructure that consists of a few SNs (i.e., reconfigurable optical add drop multiplexer (ROADM)) and the SFLs (i.e., fiber links) that interconnect the SNs. In each ROADM, the optical cross connector (OXC) is responsible for forwarding and switching lightpaths provisioned for VOLs. Those vTPs (i.e., TP slices) are created for VNs by partitioning and/or aggregation of the virtualized TPs. Each vTP can serve a single end-to-end elastic lightpath, and each created vTP can be independently operated, controlled and managed by individual VON control and management plane.

Fig. 1 also shows an example of our virtualized TP design, which is composed of a subcarrier (SC) pool, a modulator pool and a $n \times n$ bandwidth-varied spectrum selective switch (BV-SSS). The BV-SSS enables the detachment of both pools. The SC pool contains one or multiple multi-wavelength source laser (MwSL), which can generate a group of optical SCs. The modulator pool contains a collection of different types of optical modulators, offering the ability of adaptive selection of any optical modulator. Different modulation formats with adjustable baud-rates are available in the modulator pool and the total number for each type of modulators is also a finite value. Note that both resource pools

in the virtualized TP structure are completely detached by the BV-SSS. The design can offer more flexibility in the combination of available multi-dimensional resources. In addition, a “virtualized TP information” module enables procurement of up-to-date resource utilization and availability information from both resource pools through lower-level transmission protocols. An SDN agent module receives control instructions via extended OpenFlow protocol from the SDN controller in the control layer.

B. CONTROL LAYER

This layer is in charge of the control of the devices in the infrastructure layer, with two function modules, i.e., the offline/online iVONE algorithm module, and the elastic link & spectrum information module. The former decides which resources are selected to serve the incoming VON request from the SC pool and modulator pool within the virtualized TPs, and from all the SFLs and their FSs of the substrate EON, respectively. The specific offline/online iVONE algorithms will be discussed later in Section V. The latter module is also typically called as traffic engineering database (TED), which records the resource already-occupied by the operating VON requests and maintains the infrastructure status, covering the RvEON network topology, the SFL availability information and the spectrum utilization of these SFLs.

In Figure 1(b), when multiple VON requests from the service layer arrive the SDN controller, the offline/online iVONE algorithm module will firstly obtain all the requirements of each VON request, including the VON topology and bandwidth requirement, etc. Meanwhile, the SDN controller obtains the elastic link & spectrum information from the TED to prepare for the resource assignment. It involves the substrate network topology, and spectrum slot utilization of the available SFLs. As the third input of the algorithm, the virtualized TP information module collects the available TP status for both the SC pool and modulator pool, and sends them into the algorithm. Then, the algorithm module can output the decision result on how to create the infrastructure slices to serve these incoming VON requests, according to the constantly-updated resource status from the above three information modules. The decision result includes which SNs are selected for VN mapping, which routing paths and the corresponding spectrum slots are provisioned for VOLs, and which vTPs are created from both pools with the virtualized TPs, in order to accommodate each VON request. Note that the subcarrier range to be occupied by this VON keeps consistent with the spectrum range in all SFLs served for the same VON request. To create vTPs, the type of modulation format is decided as well as their baud-rate. Since all involved resources in the substrate RvEON are not infinite, the decision results obtained by the algorithm become critical to optimize the resource utilization. Finally, the decision results are passed by using extended OpenFlow protocol to the SDN agent in the infrastructure layer, which will activate the corresponding hardware devices in the RvEON, including

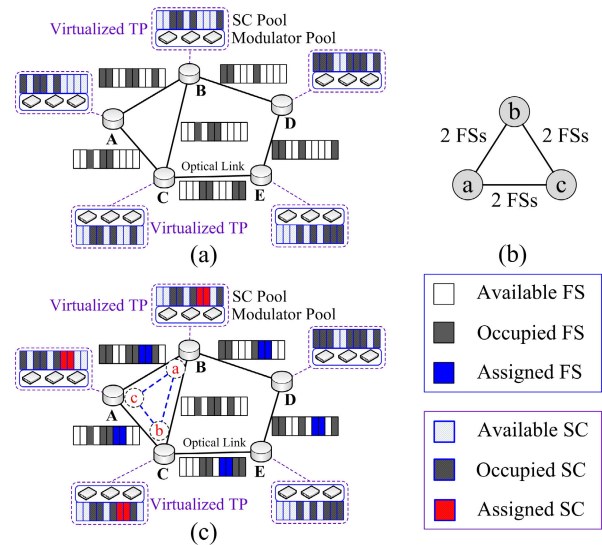


FIGURE 2. Examples of the transparent VONE. (a) Substrate RvEON. (b) Transparent VON request. (c) Transparent VONE result.

the SC and modulator pools, and OXCs within the ROADM nodes.

C. SERVICE LAYER

This layer is the place where clients access the RvEON to request for an infrastructure slice to accommodate each VON request. Some high-level administrative tasks such as client authentication and request admission, will be accomplished too in this layer.

III. PROBLEM DESCRIPTIONS

A. VONE MODELS

- 1) *Substrate RvEON*: The substrate RvEON is modeled as an undirected graph denoted as $G^s(N^s, L^s)$, where N^s is the set of SNs and L^s represents the set of SFLs. Within each SN $n^s \in N^s$, the virtualized TPs are placed to transmit and receive optical subcarriers from/to a SC pool, and various types of the modulators are available in a modulator pool. For clarification, in Figure 2(a) we define a bit-mask $b_{l^s}^s$ that contains B^s bits for each SFL $l^s \in L^s$, where B^s denotes the maximum number of FSs that a SFL can accommodate. When $b_{l^s}^s[i] = 1$, the i -th FS on the link l^s is occupied, otherwise $b_{l^s}^s[i] = 0$. Similarly, a bit-mask $b_{n^s}^s$ with the B^s bits is also defined to describe the SC resource in SNs, where B^s also denotes the maximum number of SCs that a SN can generate. When $b_{n^s}^s[j] = 1$, the j -th SC on the n^s is occupied, otherwise $b_{n^s}^s[j] = 0$. Note that the SC pool in each SN covers the same spectrum range as supported in the SFL.
- 2) *VON Requests*: The i -th VON can also be modeled as an undirected graph $g^{vi}(N^{vi}, L^{vi})$, where N^{vi} is the set of all VNs, and L^{vi} represents the set of all VOLs in the VON request g^{vi} . We use notation $b(g^{vi})$ to denote the VON bandwidth requirement in term of bit-rate.

B. TRANSPARENT VON EMBEDDING PROCEDURE

As we know, the VONE process can be also categorized into transparent and opaque scenarios [11], [13]. In this paper, we only consider a transparent VONE. We assume that there are no all-optical or optical-to-electrical-to-optical (O/E/O) spectrum converters in the RvEON. To ensure all the VOLs in a VON can be established all-optically, we need to make sure that all the VOLs in a VON occupy the same FS resources on SFLs, which is the so-called “the spectral continuity constraint.” The same assumption was also made in previous works [11], [13]. On the contrary, opaque VONE does not have this spectral continuity constraint for all VOLs. Moreover, all the VNs in a VON need to generate the SCs with the same spectrum range as that of the FSs in the assigned SFLs.

Figure 2(b) shows a transparent VON request, where the numbers on the VOLs are the bandwidth requirement $bw(g^{vi})$ measured in the number of the FSs. We assumed that all the VNs in a VON request are served by only one type of modulator. Thus the $bw(g^{vi})$ in the term of the FSs can be calculated by using the bit-rate $b(g^{vi})$ divided by the spectral utilization $SU(m^k)$ that the k -th type modulator m^k can provide. Figure 2(c) shows the results of resource allocation after embedding the VON request successfully. The assigned SCs within the SNs are marked as red slots and the assigned spectrum FSs on SFLs are blue slots.

As shown in Figure 3(a), using the traditional two-phased VONE [7], all the VNs must be mapped in the first phase, while the VOL mapping is performed in the second phase. The two mapping procedures are independent of each other. The node mapping is $\{a \rightarrow B, b \rightarrow C, c \rightarrow A\}$, while the link mapping is $\{(a, b) \rightarrow (B-D-E-C), (a, c) \rightarrow (B-A), (b, c) \rightarrow (A-C)\}$.

Figure 3(b) shows an example of the proposed integrated VONE, in which the node mapping and the link mapping are performed in an integrated way. Once a new VN is embedded, the iVONE will succeed to map all the VOLs that connect the new VN and all already-embedded VNs. Specifically, at the beginning, the VN-a is mapped onto SN-B and then the VN-b is mapped onto SN-C. Just after the VN-b embedding, the VOL (a, b) is mapped onto lightpath (B-D-E-C). Next, the VN-c is mapped onto SN-A. Since there exist two VOLs from the new VN-c to the VN-a and VN-b, respectively, the virtual link mapping $(a, c) \rightarrow (B-A)$ and $(b, c) \rightarrow (A-C)$ are performed in turn. It is observed from the iVONE procedure that the two mapping procedures would interact to each other.

IV. ILP FORMULATION

In this section, we formulate a novel ILP model for the transparent VONE over the RvEONs. To the best of our knowledge, we are the first to formulate an ILP model for multiple VON requests with the consideration of the SCs and modulators of virtualized TPs within each SN.

Parameters:

- 1) $G^s(N^s, L^s)$: The substrate EON infrastructure.
- 2) $g^{vi}(N^{vi}, L^{vi})$: The VON request.
- 3) $n(l^s)$: The number of links $l^s \in L^s$ in G^s .

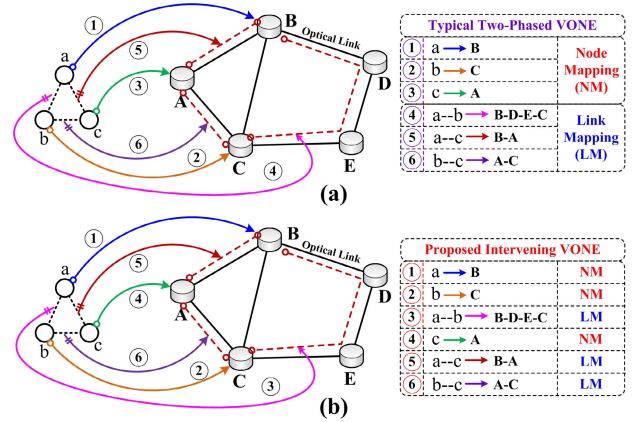


FIGURE 3. (a) Examples of the typical two-phased VONE. (b) Example of the proposed integrated VONE, where the node mapping (NM) and the link mapping (LM) are performed in an integrated way.

- 4) $b(g^{vi})$: The bit-rate requirement of the i -th VON request.
- 5) $SU(m^k)$: The spectral utilization of the k -th type modulator.
- 6) $n(m^k)$: The total number of the k -th type modulator $m^k \in M$.
- 7) $bw(g^{vi})$: The bandwidth demand measured in the number of FSs for the i -th VON request.
- 8) $Len(u^s, w^s)$: The fiber length of SFL $(u^s, w^s) \in L^s$.
- 9) $TR(m^k)$: The transmission reach of the k -th type modulator m^k can support.
- 10) F : A very large value.

Variables:

- 1) $S_{fs}(g^{vi})$: An integer variable that denotes the starting FS index of the i -th VON request.
- 2) $E_{fs}(g^{vi})$: An integer variable that denotes the ending FS index of the i -th VON request.
- 3) $S_{sc}(g^{vi})$: An integer variable that denotes the starting SC index of the i -th VON request.
- 4) $E_{sc}(g^{vi})$: An integer variable that denotes the ending SC index of the i -th VON request.
- 5) $\delta_{fs}(g^{vi}, g^{vj})$: A boolean variable that takes the value of zero if the FS index $E_{fs}(g^{vj})$ of the j -th VON request is smaller than the starting FS index $S_{fs}(g^{vi})$ of the i -th VON request. This notation makes sense only when two different VON requests share common link(s).
- 6) $\delta_{sc}(g^{vi}, g^{vj})$: A boolean variable that takes the value of zero if the SC index $E_{sc}(g^{vj})$ of the j -th VON request is smaller than the starting SC index $S_{sc}(g^{vi})$ of the i -th VON request. This notation makes sense only when two different VON requests share same SN.
- 7) $vnsn(n^{vi}, n^s)$: A boolean variable that equals 1 if the VN n^{vi} of the i -th VON request is mapped onto the SN n^s .
- 8) $volsfl((u^{vi}, w^{vi}), (u^s, w^s))$: A boolean variable that equals 1 if the VOL (u^{vi}, w^{vi}) of the i -th VON request is mapped onto the SFL (u^s, w^s) .

- 9) $\delta(g^{vi}, m^k)$: A boolean variable that equals 1 if the i -th VON request is served with the k -th type modulator m^k .
- 10) $mn(g^{vi})$: The number of the VNs in the i -th VON request.
- 11) $c(u^s, w^s)$: The maximal index of used FSs on each SFL $(u^s, w^s) \in L^s$.
- 12) $C_{average}^s$: The average value of the maximum used FSs on all SFLs.

Objective:

$$\text{Minimize } C_{average}^s$$

Our objective is to minimize the average number of the maximum used FSs in the entire network, which tries to improve the FS utilization from an overall point of view.

Constraints:

$$bw(g^{vi}) = b(g^{vi}) / (SU(m^k) \times C_{slot}) + N_{GB} - F \\ \times (1 - \delta(g^{vi}, m^k)), \\ \forall g^{vi} \in G^{vi}, \forall m^k \in M \quad (1)$$

Equation (1) calculates the requested FSs of each VON request based on the adopted k -th type modulator $m^k \in M$. The C_{slot} denotes the frequency range (i.e., 12.5GHz) of one FS. The N_{GB} is guard band in term of the FSs.

a) Node mapping constraints

$$\sum_{n^s \in N^s} vnsn(n^{vi}, n^s) = 1, \forall g^{vi} \in G^{vi}, \forall n^{vi} \in N^{vi} \quad (2)$$

$$\sum_{n^{vi} \in N^{vi}} vnsn(n^{vi}, n^s) \leq 1, \forall g^{vi} \in G^{vi}, \forall n^s \in N^s \quad (3)$$

Equations (2) and (3) ensure that each VN in a VON request is mapped onto a unique SN.

b) SC and modulator constraints

$$\delta_{sc}(g^{vi}, g^{vj}) + \delta_{sc}(g^{vj}, g^{vi}) = 1, \forall g^{vi}, g^{vj} \in G^{vi}, g^{vi} \neq g^{vj} \quad (4)$$

$$E_{sc}(g^{vj}) - S_{sc}(g^{vi}) \leq F \\ \times \left(\frac{\delta_{sc}(g^{vi}, g^{vj}) + 2 - vnsn(n^{vi}, n^s)}{-vnsn(n^{vj}, n^s)} \right) - 1, \\ \forall g^{vi}, g^{vj} \in G^{vi}, g^{vi} \neq g^{vj}, \forall n^{vi} \in N^{vi}, \forall n^{vj} \in N^{vj}, \forall n^s \in N^s \quad (5)$$

Equations (4) and (5) ensure both of the *constraints of SC continuity and SC contiguous* within each SN, and satisfy the *SC non-overlap* requirement for different VNs that share same SN. In other words, when two VNs n^{vi} and n^{vj} in two different VON requests share common SN, the assigned SCs of n^{vi} can be either before or after the SCs of n^{vj} . In particular, if n^{vi} and n^{vj} share a common SN n^s , i.e., $vnsn(n^{vi}, n^s) = vnsn(n^{vj}, n^s) = 1$ and $\delta_{sc}(g^{vi}, g^{vj}) = 0$, then $S_{sc}(g^{vi}) \geq E_{sc}(g^{vi}) + 1$ can be obtained; otherwise, the inequality (5)

always holds.

$$\sum_{m^k \in M} \delta(g^{vi}, m^k) = 1, \forall g^{vi} \in G^{vi} \quad (6)$$

$$\sum_{g^{vi} \in G^{vi}} \delta(g^{vi}, m^k) \times mn(g^{vi}) \leq n(m^k), \forall m^k \in M \quad (7)$$

Equations (6)-(7) ensure that each VON request is served with only one type of the modulator, and the number of the used modulators for all VON requests should not exceed the total number of the available modulators per type.

c) Link mapping constraints

$$\sum_{(u^s, w^s) \in L^s} volsfl((u^{vi}, w^{vi}), (u^s, w^s)) \\ - \sum_{(w^s, u^s)} volsfl((u^{vi}, w^{vi}), (w^s, u^s)) \\ = vnsn(u^{vi}, w^s) - vnsn(w^{vi}, w^s) \\ \forall g^{vi} \in G^{vi}, \forall (u^{vi}, w^{vi}) \in L^{vi}, \forall w^s \in N^s \quad (8)$$

Equation (8) is the flow conservation constraint. This constraint ensures that on all the SNs, the total number of the in-flows equals to that of the out-flows, except for the embedded SNs for the end-nodes of the VOL. This ensures a unique route of the lightpath established for one specific VOL.

$$\sum_{(u^{vi}, w^{vi}) \in L^{vi}} volsfl((u^{vi}, w^{vi}), (u^s, w^s)) = 1, \\ \forall g^{vi} \in G^{vi}, \forall (u^s, w^s) \in L^s \quad (9)$$

Equation (9) ensures that for all the VOLs in the same VON g^{vi} , their embedded lightpaths in the substrate RvEON are link-disjoint.

$$volsfl((u^{vi}, w^{vi}), (u^s, w^s)) = volsfl((u^{vi}, w^{vi}), (w^s, u^s)) \\ \forall g^{vi} \in G^{vi}, \forall (u^s, w^s) \in L^s, \forall (u^{vi}, w^{vi}) \in L^{vi} \quad (10)$$

Equation (10) ensures that all the VOLs in any VON request are undirected.

$$\delta_{fs}(g^{vi}, g^{vj}) + \delta_{fs}(g^{vj}, g^{vi}) = 1, \forall g^{vi}, g^{vj} \in G^{vi}, g^{vi} \neq g^{vj} \quad (11)$$

$$E_{fs}(g^{vi}) - S_{fs}(g^{vi}) \leq F \\ \times \left(\frac{\delta_{fs}(g^{vi}, g^{vj}) + 2 - volsfl((u^{vi}, w^{vi}), (u^s, w^s))}{-volsfl((u^{vj}, w^{vj}), (u^s, w^s))} \right) - 1, \\ \forall g^{vi}, g^{vj} \in G^{vi}, g^{vi} \neq g^{vj}, \forall (u^s, w^s) \in L^s, \\ \forall (u^{vi}, w^{vi}) \in L^{vi}, \forall (u^{vj}, w^{vj}) \in L^{vj} \quad (12)$$

Equations (11) and (12) ensure both of the *constraints of FS continuity and FS contiguous* for each VOL, and satisfy the *FS non-overlap* requirement between different VOL that share common link(s). In other words, when two VON requests share common link(s), the assigned FSs of

one VON can be either before or after the FSs of the other VON. In particular, if two VOLs (u^{vi}, w^{vi}) and (u^{vj}, w^{vj}) from two different VONS share a common SFL (u^s, w^s) , i.e., $\text{volssl}((u^{vi}, w^{vi}), (u^s, w^s)) = \text{volssl}((u^{vj}, w^{vj}), (u^s, w^s)) = 1$ and $\delta_{fs}(g^{vi}, g^{vj}) = 0$, then we can obtain $S_{fs}(g^{vi}) \geq E_{fs}(g^{vj}) + 1$; otherwise, the inequality (12) always holds.

$$\sum_{(u^s, w^s)} \delta(g^{vi}, m^k) \times \text{volssl}((u^{vi}, w^{vi}), (u^s, w^s)) \times \text{Len}(u^s, w^s) \leq TR(m^k), \forall g^{vi} \in G^{vi}, \forall (u^s, w^s) \in L^s, \forall (u^{vi}, w^{vi}) \in L^{vi} \quad (13)$$

Equation (13) ensures that the fiber length of the mapped SFL(s) for a specific VOL should not exceed the transmission reach of the k -th type modulator $m^k \in M$.

d) Other constraints

$$E_{sc}(g^{vi}) = E_{fs}(g^{vi}), \forall g^{vi} \in G^{vi} \quad (14)$$

$$S_{sc}(g^{vi}) = S_{fs}(g^{vi}), \forall g^{vi} \in G^{vi} \quad (15)$$

$$E_{fs}(g^{vi}) = S_{fs}(g^{vi}) + bw(g^{vi}) - 1, \forall g^{vi} \in G^{vi} \quad (16)$$

$$c(u^s, w^s) \geq E_{fs}(g^{vi}) \times \text{volssl}((u^{vi}, w^{vi}), (u^s, w^s)) \quad (17)$$

$$\forall (u^{vi}, w^{vi}) \in L^{vi}, \forall (u^s, w^s) \in L^s$$

$$C_{average}^s = \sum_{(u^s, w^s) \in L^s} c(u^s, w^s) / n(l^s) \quad (18)$$

Equations (14)-(15) ensure that the FS resources on SFLs and the SC resources within SNs served by each VON request use the same starting and ending index. Equation (16) ensures that the ending FS index of one VON is equal to the starting slot index of the VON plus the number of FSs required by the VON request. Equation (17) ensures that the maximal index $c(u^s, w^s)$ of the used FSs on one SFL (u^s, w^s) is not smaller than the ending FS index of any VON. Equation (18) calculates the average value $C_{average}^s$ of the maximum used FSs on all SFLs.

V. HEURISTIC OFFLINE AND ONLINE ALGORITHMS

The developed ILP model can get the optimal solution for the VONE and arrange the FS/SC utilization in the most compact way. But the ILP model would be unable to provide a scalable solution in a reasonable time for large-scale networks, since they have to search within the whole solution space to obtain the optimal solution. Thus, the execution time and computational complexity of the ILP model will increase dramatically with the increase of the network scale. Therefore, we propose time-efficient offline and online heuristic algorithms for the transparent iVONE over the RvEONs. The iVONE algorithm performs the node mapping and link mapping in an integrated way, instead of two-phased method. More specifically, whenever a new VN is mapped onto a SN, the algorithm will succeed to map all the VOLs that connect the new VN to those already-embedded VNs. Only if the lightpaths of these VOLs are mapped successfully on the SFLs, the new VN can

Algorithm 1 VAG Construction

Input: $G^s(N^s, L^s)$, $bw(g^{vi})$, f as the VAG's index
Output: G_{sub}^f as the f -th sub-layer VAG

- 1 $G_{sub}^f = G^s$;
- 2 Get the bit-mask on all the SNs and SFLs in G_{sub}^f ;
- 3 **For all** $l^s \in L^s$ in G^s **do**
 $f+bw(g^{vi})-1$
- 4 **If** $\sum_{j=f} b_{l^s}^s[i] > 0$
- 5 Remove the SFL l^s in G_{sub}^f ;
- 6 **End**
- 7 **End**
- 8 **For all** $n^s \in N^s$ in G^s **do**
 $f+bw(g^{vi})-1$
- 9 **If** $\sum_{j=f} b_{n^s}^s[i] > 0$
- 10 Remove the SN n^s in G_{sub}^f ;
- 11 **End**
- 12 **End**

be viewed to be mapped successfully. Otherwise, the new VN tries to be remapped onto another SN, and all the corresponding VOLs try to be remapped once again.

We first introduce a VAG method, which decomposes the substrate RvEONs into several layered graphs, according to the bandwidth requirement of the VON request, to facilitate the allocation of the link, modulator and spectrum resources.

A. VIRTUAL AUXILIARY GRAPH

For an incoming VON request, we first convert its bit-rate requirement $b(g^{vi})$ into the number of required FSs' $bw(g^{vi})$, according to the spectrum range C_{slot} of one FS and the spectral utilization $SU(m^k)$ of the adopted k -th type modulator, as shown in Eq. (19).

$$bw(g^{vi}) = \left\lceil \frac{b(g^{vi})}{SU(m^k) \times C_{slot}} \right\rceil + N_{GB}, \quad (19)$$

where the N_{GB} is the guard-band in term of FSs between two adjacent lighthpath connections on a common SFL.

Then, we transform the substrate RvEONs into several layered graphs, by means of scanning both the SC utilization of all the SNs and the FS utilization of all the SFLs. In particular, in order to build the f -th layer VAG, this approach checks whether the contiguous resource block covering f -th to $(f + bw(g^{vi}) - 1)$ -th SCs and FSs exists on each SN and SFL, respectively. If the contiguous resource block exists both on an SN n^s and SFL l^s , the n^s and l^s will be inserted into the f -th layer which is denoted as G_{sub}^f ; otherwise, the n^s and/or l^s will be removed. The details of the VAG approach are explained in Algorithm 1.

B. RMS² A SOLUTION OVER A RVEON SUB-LAYER

After obtaining a new SN u^s as candidate from the head-of-line (HOL) of the all unmarked available SNs, we design a routing, modulation, spectrum and subcarrier assignment

Algorithm 2 RMS²A Algorithm

Input: f -th G_{sub}^f , adopted m^k , existing SN w^s and new SN u^s

Output: VOL status $VOLS$

- 1 $VOLS = \text{SUCCEEDED}$;
- 2 Get transmission reach $TR(m^k)$ of the adopted k -th type modulator m^k ;
- 3 Get three shortest paths that not exceed $TR(m^k)$ between w^s and u^s in G_{sub}^f ;
- 4 **If** exists only one candidate path
- 5 Get the candidate p_{can} as selected substrate path;
- 6 **End**
- 7 **If** exists multiple candidate paths p_{can}
- 8 Get the candidate(s) p_{can_minL} that has shortest path distance;
- 9 **If** exists multiple candidates p_{can_minL} with the same shortest path distance
- 10 Get the candidate p_{can_minU} with the lowest path utilization;
- 11 **End**
- 12 **End**
- 13 **If** the path cannot be found
- 14 **Return**($VOLS = \text{FAILED}$);
- 15 **End**
- 16 **Return**($VOLS$);

(RMS²A) algorithm to setup lightpaths for all the VOLs between the new SN u^s and all existing SN w^s that has accommodated a VN of the VON. First, we can obtain the transmission reach $TR(m^k)$ of the k -th modulator m^k . Then, in a certain sub-layer G_{sub}^f , three shortest lightpaths at most for the (u^s, w^s) node pair will be found whose transmission reach should not exceed the $TR(m^k)$. If there are multiple lightpath candidates, then final allocation will choose the candidate p_{can_minL} that has the shortest path distance. If more than one candidate has the same shortest path distance, then the one has the lowest path spectrum utilization p_{can_minU} will be selected. Algorithm 2 explains the details of the RMS²A algorithm.

C. INTEGRATED VONE ALGORITHMS

Based on the proposed VAG method and RMS²A algorithm, we design *iVONE* algorithms for both offline and online scenarios.

1) Offline iVONE Algorithm

For the offline scenario, we assume that all the VONs with the specific bit-rate requirement $b(g^{vi})$ are generated randomly in advance. For each VON, we define a parameter (i.e., average bandwidth) $\overline{BW}(g^{vi})$ to measure their priority in the offline scenario:

$$\overline{BW}(g^{vi}) = b(g^{vi}) \times \left(\sum_{n^{vi} \in N^{vi}} \beta(n^{vi}) \right) / nvn(g^{vi}), \quad (20)$$

Algorithm 3 Offline Integrated VONE Algorithm

- 1 **Sort** all the VON requests in descending order based on their $\overline{BW}(g^{vi})$
- 2 **For** each VON request
- 3 Get the bit-rate $b(g^{vi})$ of the VON request g^{vi} ;
- 4 **For** all the available modulators in descending order of their modulation level **do**
- 5 Calculate $bw(g^{vi})$, according to $b(g^{vi})$ and $SU(m^k)$;
- 6 **For** $f = 1$ to $T-bw(g^{vi})+1$ **do**
- 7 Build f -th VAG G_{sub}^f with Algorithm 1;
- 8 Calculate node degree $\beta(u^s)$ for each SN in G_{sub}^f ;
- 9 Calculate node degree $\beta(u^v)$ for each VN in g^{vi} ;
- 10 **For** all VNs in descending order of $\beta(u^v)$ **do**
- 11 $VS = \text{FAILED}$;
- 12 **For** all unmarked SNs in descending order of their $\beta(u^s)$ **do**
- 13 Get a new u^s as candidate from head-of-line
- 14 **If** $\beta(u^s) \geq \beta(u^v)$
- 15 **For** all already-embedded VNs w^v in g^{vi} **do**
- 16 **If** there exists a VOL between the new u^v and the already-embedded w^v in g^{vi}
- 17 Apply Algorithm 2 for the VOL;
- 18 **If** $VOLS = \text{FAILED}$
- 19 **break**;
- 20 **Else** continue the loop
- 21 **Else** continue the loop
- 22 $VS = \text{SUCCEED}$;
- 23 **Else** continue the loop
- 24 **If** $VS = \text{FAILED}$
- 25 **break**;
- 26 **Else if** $VS = \text{SUCCEED}$
- 27 Map VN u^v onto SN u^s ;
- 28 Map all VOLs (u^v, w^v) onto SFLs (u^s, w^s) ;
- 29 Mark SN u^s , SFL (u^s, w^s) as selected and **break**;
- 30 **Update** available resource;
- 31 **End**
- 32 **If** $VS = \text{FAILED}$
- 33 Mark g^{vi} as blocked and **break**;
- 34 **Else** continue the loop
- 35 **End**
- 36 **End**
- 37 **End**
- 38 **End**
- 39 Mark g^{vi} as blocked;
- 40 **Return** ($VS = \text{FAILED}$);

where the $\beta(n^{vi})$ is the degree of the node n^{vi} of the set N^{vi} , and $nvn(g^{vi})$ is the number of the VNs within the VON g^{vi} .

These VON requests will be provisioned one by one in the descending order of their $\overline{BW}(g^{vi})$. For each VON request, firstly, all the available modulators are ranked in descending order of modulation level. Thus, the modulator with the higher modulation level would be given priority for usage,

Algorithm 4 Online Integrated VONE Algorithm

Input: Substrate network G^s , VON request g^{vi}
Output : VONE status VS

- 1 Get the arrival time $AT(g^{vi})$ of the VON request g^{vi} ;
- 2 $T_{current} = AT(g^{vi})$;
- 3 **If** $V_{provisioned}$ is not NULL **then**
- 4 **For each** $g^{vj} \in V_{provisioned}$
- 5 **If** $AT(g^{vj}) + \Delta T(g^{vj}) \leq T_{current}$ **then**
- 6 Release the occupied resources and remove the VON request g^{vj} from the set $V_{provisioned}$;
- 7 **End**
- 8 **End**
- 9 **Call** steps 3-34 from Algorithm 3;
- 10 **If** $VS = \text{SUCCEEDED}$
- 11 Mark g^{vi} as allocated and update resource in G^s ;
- 12 The g^{vi} is put into the set $V_{provisioned}$, and its status is set to be waiting for releasing at time $AT(g^{vi}) + \Delta T(g^{vi})$;
- 13 **End**
- 14 Mark g^{vi} as blocked;
- 15 **Return** ($VS = \text{FAILED}$);

since its spectral utilization is higher. Then, in order to reduce the computational complexity, we adopt first-fit policy to build VAG with Algorithm 1. On certain sub-layer VAG, whenever a new VN tries to be mapped onto a candidate SN, the algorithm immediately in turn maps those VOLs that connect this new VN to the already-embedded VNs in line 15 - 23, where the TR constraints of the available modulators in the SN will be taken into the account in the link mapping. It can be seen that for the VONE, the node mapping and link mapping are performed in an integrated way. Each time a VON provisioned, the assigned SCs and modulators within the vTPs and spectrum FSs on SFLs are occupied and will never be released (see line 27 - 29). Otherwise, the next sub-layer VAG will be built until an eligible sub-layer VAG is found. The overall procedures of the offline iVONE algorithm are described at length in Algorithm 3.

2) *Online iVONE Algorithm*

Under the online scenario, each VON request undergoes a birth-and-death process, i.e., arriving sequentially and randomly, holding for a certain time, and finally departing, releasing the occupied resources covering spectrum slots in SFLs, and SCs and modulators of the vTPs in corresponding SNs. The arrival time and lifetime of each VON request are denoted as $AT(g^{vi})$ and $\Delta T(g^{vi})$. The initial time point is defined as the starting time of the first VON request to arrive and is represented as $T_{current}$. The set of all the already provisioned VON requests are represented as $V_{provisioned}$. When the i -th VON request arrives at the time $AT(g^{vi})$, we assume the mapping process will be executed immediately. Before the i -th VON request arrives, the algorithm will check whether it is time to release those already-embedded VON requests automatically. If any of these VON requests have

a lifetime that is about to expire, the occupied resources of the SCs and modulators of the vTPs in SNs and FS resources on SFLs will be released immediately after the lifetime of this VON request expires. Also, the FS/SC indexes associated with the released lightpaths and the vTPs will be updated respectively to accommodate next VON request. Then the i -th VON request starts to be provisioned. If the i -th VON request is successfully provisioned, the status of this VON request will be set as the status of “waiting for releasing”, and will be put into the set $V_{provisioned}$. Algorithm 4 describes the overall online iVONE algorithm in detail.

D. TIME COMPLEXITY ANALYSIS

The time complexities of the proposed algorithms are analyzed as follows.

In the VAG method, the $(B^s - bw(g^{vi}) + 1)$ sub-layers are created, and hence the time complexity of the VAG algorithm is $\Gamma = O((B^s - bw(g^{vi}) + 1) \cdot (|L^s| + |N^s|))$.

In the integrated node and link mapping algorithm, at first the complexity of the Dijkstra algorithm on a sub-layer is $\Delta = O(|N^s| + |N^s|(|N^s| - 1) + |N^s| \log 2 |N^s|)$ [20], and then the time complexity of sorting node degree of SNs and VNs are $O(|N^v|^2)$ and $O(|N^s|^2)$, respectively. Thus the time complexity of the integrated node and link mapping algorithm is $O(|N^s|^2 + |N^v|^2 + |N^s| \cdot |L^v| \cdot \Delta)$.

Finally, the overall time complexity of the integrated VONE algorithm is

$$|M| \cdot \left[\Gamma + O(|N^s|^2 + |N^v|^2 + |N^s| \cdot |L^v| \cdot \Delta) \right],$$

where $|M|$ denotes the number of modulator types in the substrate RvEONs.

VI. SIMULATION RESULTS

In this section, we perform offline and online simulations to evaluate the performance of the proposed algorithms and investigate how the impact of the VON request bit-rate, the different configurations of various modulators that each vTP can offer on the network performances. Two different types of VON requests are applied in the simulations. The first type of requests is randomly generated including five groups. The request bit-rate lower-bound of each group is varied between 20 to 100 Gb/s in spacing of 20 Gb/s, while the upper-bound is fixed to be 200Gb/s. Thus, the five groups of requests are the ranges of [20, 200], [40, 200], [60, 200], [80, 200], [100, 200] Gb/s, respectively. In the second type, other five groups of requests are generated with varying lower- and upper- bounds of the bit-rate $b(g^{vi})$, which are the ranges of [20, 40], [40, 80], [80, 120], [120, 160], [160, 200] Gb/s, respectively.

A small-scale five-node network and a large-scale network topology NSFNET are used in the simulations as shown in Figure 4. In the figure, the numbers on the line represent link length in kilometers. In our simulations, four formats of the used modulators are assumed as BPSK, QPSK, 8QAM, and 16QAM. The transmission reaches (TRs) of the BPSK,

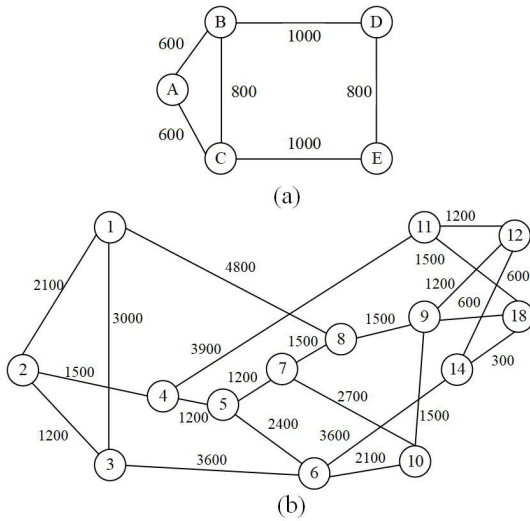


FIGURE 4. Topologies used in simulations with fiber length in kilometers marked on links. (a) The five-node topology. (b) The NSFNET topology.

TABLE 1. Simulation parameters [21].

Parameter	Value
T, number of frequency slots per link	320
BW_{slot} , bandwidth of a frequency slot	12.5GHz
C_{slot} , capacity of a frequency slot with $lev = 1$	12.5Gb/s
N_{GB} , number of slots for guard-band per connection	1
Transmission reach of BPSK ($lev = 1$)	9600 km
Transmission reach of QPSK ($lev = 2$)	4800 km
Transmission reach of 8QAM ($lev = 3$)	2400 km
Transmission reach of 16QAM ($lev = 4$)	1200 km

QPSK, 8-QAM, and 16-QAM signals are determined based on the experimental results reported in [21]. Table 1 summarizes some simulation parameters.

A. COMPARISON OF ILP MODEL AND OFFLINE HEURISTIC

We consider the average maximum used FSs $C_{average}^s$ per link to compare the performance of the ILP model and our proposed iVONE algorithm in the simple five-node network. The total numbers of four types of modulators (i.e., BPSK, QPSK, 8QAM, and 16QAM) are initialized to be 15, 12, 12 and 9, respectively. To make picture brief and clear, in Figure 5(a), we only present simulation results for three groups of requests of the first type, i.e., the ranges of [20, 200], [60, 200], [100, 200] Gb/s. In Figure 5(b), the simulation results for the second type of VON requests are given out. We can observe from both pictures that as the number of VON requests increases, the average maximum used FSs $C_{average}^s$ increases for both the ILP model and the offline algorithm. The ILP result is a bit better than that of the offline heuristic algorithm and the difference is mainly due to the incurred spectral fragments during the heuristic iVONE process. And with the increase of the request bitrates, it is apparent that the used resources become more and more too.

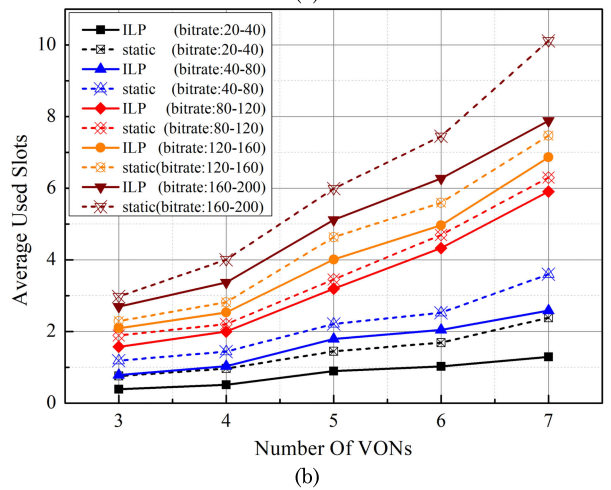
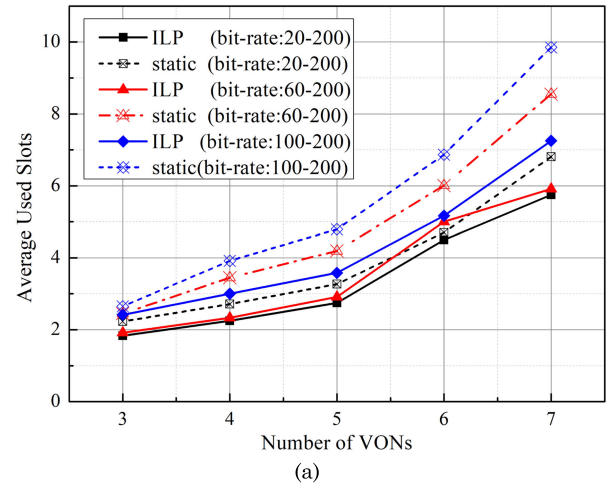


FIGURE 5. Comparison of simulation results both for ILP model with offline iVONE algorithm. (a) First types of VON requests. (b) Second type of VON requests.

B. IMPACT OF DIFFERENT MODULATOR POOLS UNDER OFFLINE SCENARIO

Then we focus on the impact of the different configuration of various types of modulators on the network performances under offline scenario by applying 100 VON requests with varying bit-rates. In our simulations, to evaluate the system performance, the spectrum utilization (SU) is defined as the time average ratio of the occupied spectrum bandwidth over the total bandwidth during the simulation period.

$$SU = \frac{\sum_{g^v \in V_{provisioned}} \sum_{l^v \in L^v} bw(g^v) \cdot \Delta T(g^v)}{\sum_{l^s \in L^s} B^s \cdot \xi(l^s) \cdot T_{total}}, \quad (21)$$

where $\xi(l^s) = 1$ represents a SFL $l^s \in L^s$ is used during the simulation period and T_{total} is the total simulation time. Note that the SU definition is a dimensionless ratio, which is more appropriate for dynamic traffic scenario. The same definition is adopted in the previous papers [22]–[24].

During the simulation, the total numbers of four types of modulators (i.e., BPSK, QPSK, 8QAM, and 16QAM) are

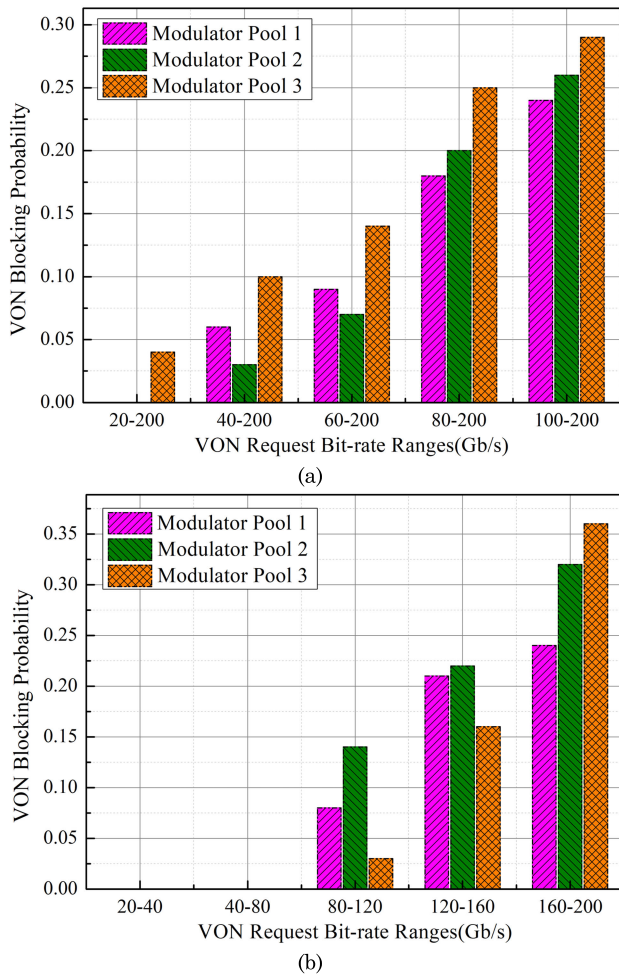


FIGURE 6. Offline simulation results of VON blocking probability. (a) First type of VON requests. (b) Second type of VON requests.

initialized to be 125, 100, 100 and 75 in turns. In Modulator Pool-1, the initial modulators types and their numbers are described as above. Modulator Pool-2 reduces the number of BPSK modulators to 75 and increases the number of QPSK and 8QAM by a quarter. Modulator Pool-3 removes all the BPSK modulators and increases the number of 8QAM and 16QAM modulators to 150 instead.

In Figure 6, it can be found clearly that as the VON bit-rate lower-bound gets larger, the request blocking probability (BP) increases for all modulator pools due to the limitation of the network resources including FSs and SCs. In Figure 6(a), for the first type of the VON requests, we can see that the modulator pool-1 and pool-2 can achieve similar BP performance, while the modulator pool-3 has the highest BP. It is because that there is no BPSK modulator in the pool-3, which can allow the longest TR as shown in Table 1. Hence, when there is no routing available that satisfies the TR constraint, the VON request will be blocked. It can be concluded that the BPSK modulator is necessary to reduce the VON request BP.

In Figure 6(b), when the bit-rate ranges are [20, 40] and [40, 80], the three modulators pools achieve the zero BP.

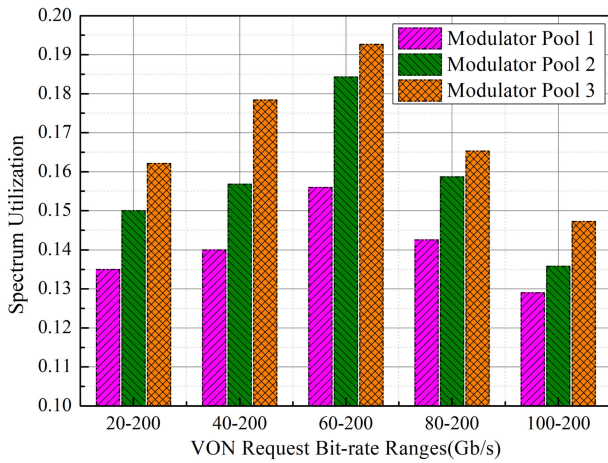
It is due to the fact that there are sufficient resources to accommodate these VON requests with the lower bit-rate requirements. As the VON bit-rate ranges achieve medium requirements, i.e., [80, 120] and [120, 160], the modulator pool-3 performs the best BP performance, the pool-1 is the better, and the pool-2 is the worst. It is because that in the modulator pool-3, the usage of the high-level modulators can facilitate to improve network spectrum utilization, and hence more free FSs are available to accommodate VON requests. In the other two pools, the pool-1 has more low-level BPSK modulators, which has larger flexibility to support more candidate paths. Hence, the modulator pool-1 performs a bit better than the pool-2 in term of the BP. When handling the bit-rate range with the highest requirement [160, 200], the pool-3 performs the worst. This is again the proof of the necessity and importance of the BPSK modulators. Although the high-level modulators inherently show superiority in the spectrum utilization, these modulators have the limited TR, which may lead to the case that some VON requests with strict TR constraints cannot be embedded successfully. Therefore, the proper introduction of lower-level modulators like BPSK will in fact increase the ability of network to handle VON requests with strict TR constraints.

Figure 7 shows the spectrum utilization (SU) of the RvEONs with different modulator pools for the different types of VON requests. We can observe that the pool-3 always achieves the largest SU and in Fig. 7(a), the pool-2 performs better than the pool-1. It is because that the high-level modulators can bring about the higher SU, which can consequentially lead to less SC and FS fragmentation within the SNs and on SFLs, respectively. In Figure 7, it is found that the SU performances rise first and descend later, as the bit-rates of the VON requests increase. It means that the larger the bit-rates of the VON requests are, the more likely the FS fragmentations can be easily introduced in the substrate RvEONs. When the bit-rates of the VON requests reach a certain value, the SC and FS fragmentations begin to have adverse impact on the network SU performances.

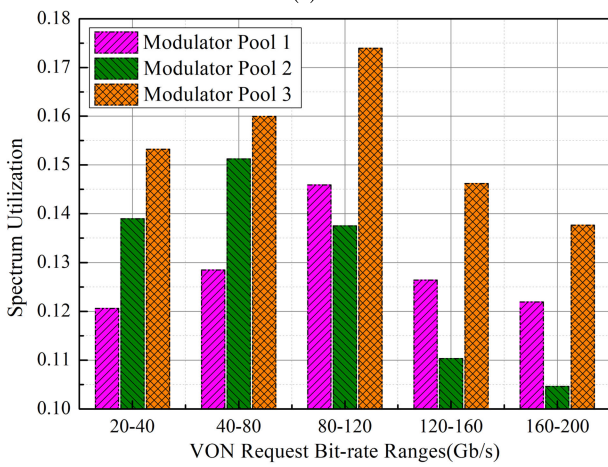
C. PERFORMANCE EVALUATION UNDER ONLINE SCENARIO

In the online simulation, we assume that the arrival of the VON request follows the Poisson traffic model. The average lifetime of each VON request $\Delta T (g^{vi})$ is assumed to be an unit time 1, which means that the value of the traffic load (i.e., $\lambda/\Delta T (g^{vi})$) equals to the request arrival rate λ . The NSFNET network topology is used in online simulations as shown in Fig. 4(b).

In Figure 8(a), we evaluate the BP performance of the proposed online integrated iVONE algorithm, compared with the benchmark two-phased algorithm in [10]. It is assumed that the number of the modulators of each type in the modulator pool is set to 100. The bit-rates of the VON requests range from 20 to 200 Gb/s. We can observe that with the increase of traffic load, the BP performances of both algorithms are on the rise, due to the limited network resources.



(a)



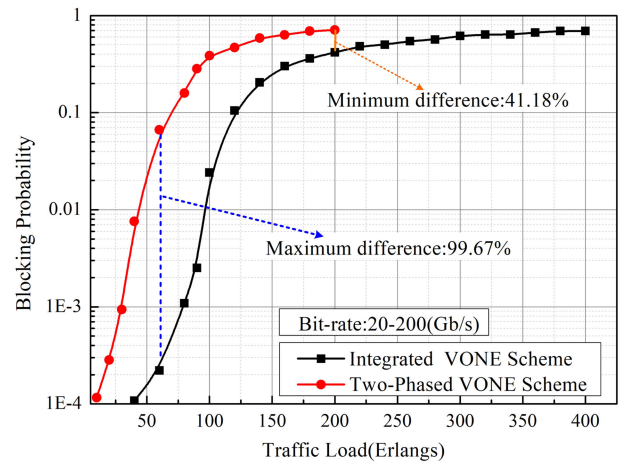
(b)

FIGURE 7. Offline simulation results of spectrum utilization. (a) First type of VON requests. (b) Second type of VON requests.

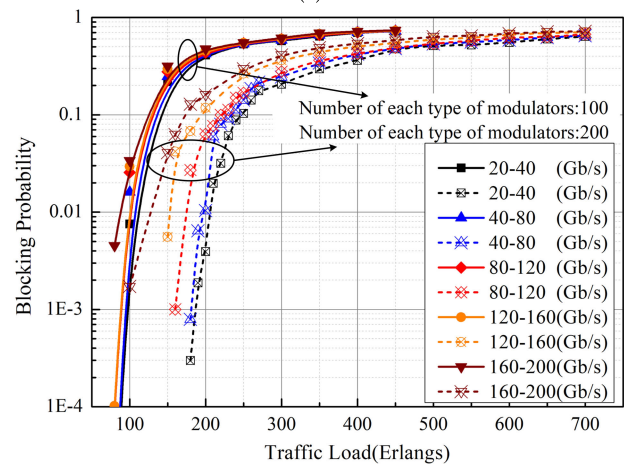
Furthermore, our algorithm can always achieve better performance in terms of BP under the same traffic load, compared with the benchmark algorithm. Our iVONE can greatly improve the BP performance by nearly 99.67 percent in the best case. It means that the proposed iVONE algorithm shows great superiority over the benchmark algorithm in terms of the BP. It can be also observed that the difference between the two algorithms becomes smaller and smaller as traffic load increases. This is mainly because as traffic load increases, there are no enough network resources available including the link, modulator and spectrum resources to accommodate newly-coming VON requests.

Then, we investigate the impact of varied VON bit-rates of the VON requests on network performance in the terms of the BP and SU. In our simulation, the number of each type of the modulators in the modulators pool is set to be 100 or 200, respectively, in order to study the effect of the different numbers of modulators on the network performance.

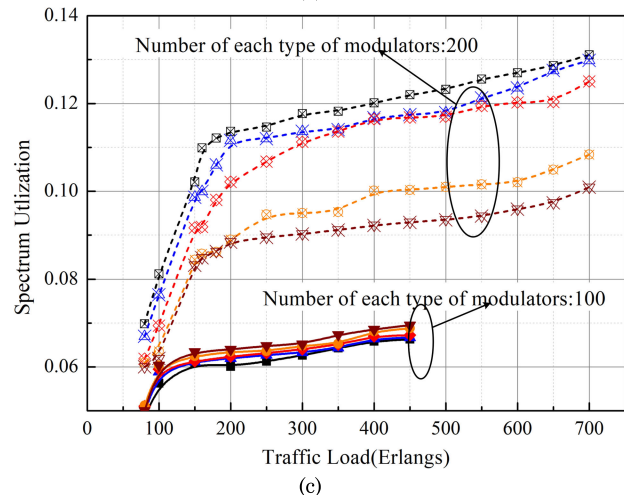
From Figure 8(b), we also find that the BP becomes larger as the traffic load increases. After the traffic load reaches a certain value, the BP gets saturated, because there are no more



(a)



(b)



(c)

FIGURE 8. Online simulation results. (a) Comparison of two algorithms. (b) The influence of factors on BP. (c) The influence of factors on SU.

resources that are available for more requests especially when the modulators have been used up. When the number of each type of modulators doubles (i.e., from 100 to 200), the request BP of the VON requests can be greatly reduced. It is because that more modulators can be available for more requests. Note that when the number of each type of modulators is

fixed to be 100, there is no apparent difference on the BP under the same traffic load, despite the bit-rate of the request varies. In this case, the modulator resources become a main limiting factor in terms of the BP. However, in the case that the number of each type of modulators is 200, the smaller the bit-rate, the lower the BP, under the same traffic load. It is due to the fact that the VON requests with the smaller bit-rate occupy the less FS and SC resources, making it easier to accommodate newly-coming VONs.

Figure 8(c) shows the SU of the substrate Rv-EONs under the different traffic loads. When the number of the modulator is 100, there is no significant difference on the SU, as the bit-rate varies. When it doubles to 200, there is a remarkable increase of the SU under the same traffic load. Another phenomenon that must be pointed out is that the lower bit-rate of the VONs usually brings about higher SU. It is because that the lower bit-rate requests always require fewer resources. As a result, it will also lead to less SC and FS fragmentation within the SNs and on SFLs, respectively, which is helpful to improve the SU.

VII. CONCLUSION

In this paper, we first introduce a new concept of RvEON, which has realized both link-tier spectrum virtualization and node-tier transponder virtualization. We then have proposed a novel iVONE scheme over the RvEONs, where the node mapping and link mapping are performed in an integrated way, which is totally different from the existing two-phased VONE scheme. A novel ILP model is also formulated, which takes into account the subcarrier and modulator resource constraints of the virtualized TPs. A novel RMS²A algorithm is designed to setup lightpaths for VOL mapping. The simulation results demonstrate that our proposed iVONE scheme can achieve better BP performance than the benchmark two-phased algorithm. Moreover, the different bit-rate ranges of VON requests and the different configurations of the modulator pool have dramatic impacts on the network performances.

REFERENCES

- [1] C. Vecchiola, S. Pandey, and R. Buyya, "High-performance cloud computing: A view of scientific applications," in *Proc. 10th Int. Symp. Pervasive Syst., Algorithms Netw.*, Kaohsiung, Taiwan, Dec. 2009, pp. 4–16.
- [2] N. M. M. K. Chowdhury and R. Boutaba, "A survey of network virtualization," *Comput. Netw.*, vol. 54, no. 5, pp. 862–876, Apr. 2010.
- [3] T. Anderson, L. Peterson, S. Shenker, and J. Turner, "Overcoming the Internet impasse through virtualization," *Computer*, vol. 38, no. 4, pp. 34–41, Apr. 2005.
- [4] S. Figuerola and M. Lemay, "Infrastructure services for optical networks," *IEEE/OSA J. Opt. Commun. Netw.*, vol. 1, no. 2, pp. A247–A257, Jul. 2009.
- [5] A. Fischer, J. F. Botero, M. T. Beck, H. de Meer, and X. Hesselbach, "Virtual network embedding: A survey," *IEEE Commun. Surveys Tuts.*, vol. 15, no. 4, pp. 1888–1906, 4th Quarter, 2013.
- [6] M. Jinno, H. Takara, B. Kozicki, Y. Tsukishima, Y. Sone, and S. Matsuoka, "Spectrum-efficient and scalable elastic optical path network: Architecture, benefits, and enabling technologies," *IEEE Commun. Mag.*, vol. 47, no. 11, pp. 66–73, Nov. 2009.
- [7] Y. Ou, A. Hammad, S. Peng, R. Nejabati, and D. Simeonidou, "Online and offline virtualization of optical transceiver," *IEEE/OSA J. Opt. Commun. Netw.*, vol. 7, no. 8, pp. 748–760, Aug. 2015.
- [8] Y. Ou, S. Yan, A. Hammad, B. Guo, S. Peng, R. Nejabati, and D. Simeonidou, "Demonstration of virtualizable and software-defined optical transceiver," *J. Lightw. Technol.*, vol. 34, no. 8, pp. 1916–1924, Apr. 15, 2016.
- [9] S. Zhang, L. Shi, C. S. K. Vadrevu, and B. Mukherjee, "Network virtualization over WDM networks," in *Proc. 5th IEEE Int. Conf. Adv. Telecommun. Syst. Netw. (ANTS)*, Bangalore, India, Dec. 2011, pp. 1–3.
- [10] S. Peng, R. Nejabati, S. Azodolmolky, E. Escalona, and D. Simeonidou, "An impairment-aware virtual optical network composition mechanism for future Internet," in *Proc. 37th Eur. Conf. Exhibit. Opt. Commun.*, Geneva, Switzerland, 2011, pp. 1–3.
- [11] A. Pagès, J. Perelló, and S. Spadaro, "Virtual network embedding in optical infrastructures," in *Proc. 14th Int. Conf. Transparent Opt. Netw. (ICTON)*, Coventry, U.K., 2012, pp. 1–4.
- [12] R. Lin, S. Luo, J. Zhou, S. Wang, A. Cai, W. Zhong, and M. Zukerman, "Virtual network embedding with adaptive modulation in flexi-grid networks," *J. Lightw. Technol.*, vol. 36, no. 17, pp. 3551–3563, Sep. 1, 2018.
- [13] A. Pagès, J. Perelló, S. Spadaro, J. A. García-Espín, J. Ferrer Riera, and S. Figuerola, "Optimal allocation of virtual optical networks for the future Internet," in *Proc. 16th Int. Conf. Opt. Netw. Design Model. (ONDM)*, Colchester, U.K., 2012, pp. 1–6.
- [14] L. Gong and Z. Zhu, "Virtual optical network embedding (VONE) over elastic optical networks," *J. Lightw. Technol.*, vol. 32, no. 3, pp. 450–460, Feb. 1, 2014.
- [15] W. Wei, H. Gu, K. Wang, X. Yu, and X. Liu, "Improving cloud-based IoT services through virtual network embedding in elastic optical inter-DC networks," *IEEE Internet Things J.*, vol. 6, no. 1, pp. 986–996, Feb. 2019.
- [16] W. Hou, Z. Ning, L. Guo, Z. Chen, and M. S. Obaidat, "Novel framework of risk-aware virtual network embedding in optical data center networks," *IEEE Syst. J.*, vol. 12, no. 3, pp. 2473–2482, Sep. 2018.
- [17] D. L. Nguyen, H. Byun, N. Kim, and C. K. Kim, "Toward efficient dynamic virtual network embedding strategy for cloud networks," *Int. J. Distrib. Sensor Netw.*, vol. 14, no. 3, 2018, Art. no. 1550147718764789.
- [18] Y. Wang, Z. McNulty, and H. Nguyen, "Network virtualization in spectrum sliced elastic optical path networks," *J. Lightw. Technol.*, vol. 35, no. 10, pp. 1962–1970, May 15, 2017.
- [19] A. Blenk, P. Kalmbach, J. Zerwas, M. Jarschel, S. Schmid, and W. Kellerer, "NeuroViNE: A neural preprocessor for your virtual network embedding algorithm," in *Proc. IEEE Conf. Comput. Commun.*, Honolulu, HI, USA, Apr. 2018, pp. 405–413.
- [20] J. Zhang, Y. Ji, M. Song, H. Li, R. Gu, Y. Zhao, and J. Zhang, "Dynamic virtual network embedding over multilayer optical networks," *IEEE/OSA J. Opt. Commun. Netw.*, vol. 7, no. 9, pp. 918–927, Sep. 2015.
- [21] A. Bocoli, M. Schuster, F. Rambach, M. Kiese, C. Bunge, and B. Spinnler, "Reach-dependent capacity in optical networks enabled by OFDM," in *Proc. Conf. Opt. Fiber Commun. Post Deadline Papers*, San Diego, CA, USA, 2009, pp. 1–3.
- [22] X. Wan, N. Hua, and X. Zheng, "Dynamic routing and spectrum assignment in spectrum-flexible transparent optical networks," *Opt. Commun. Netw., IEEE/OSA J.*, vol. 4, no. 8, pp. 603–613, Aug. 2012.
- [23] W. Lu and Z. Zhu, "Dynamic service provisioning of advance reservation requests in elastic optical networks," *J. Lightw. Technol.*, vol. 31, no. 10, pp. 1621–1627, May 15, 2013.
- [24] M. Zhu, S. Zhang, Q. Sun, G. Li, B. Chen, and J. Gu, "Fragmentation-aware VONE in elastic optical networks," *IEEE/OSA J. Opt. Commun. Netw.*, vol. 10, no. 9, pp. 809–822, Sep. 2018.

MIN ZHU is currently an Associate Professor and a Doctoral Supervisor with the National Mobile Communications Research Laboratory, Southeast University, Nanjing, China, and Purple Mountain Laboratories, Nanjing. He has published more than 50 articles in refereed journals and conferences of IEEE and OSA. His research interests include optical access networks and systems, network resource scheduling, and optimization algorithms. He also serves as an active reviewer for many international journals and conferences.

TIANYU SHEN received the B.Sc. degree from the College of Communication Engineering, Jilin University, Changchun, China, in June 2018. He is currently pursuing the M.S. degree with the School of Electronic Science and Engineering, Southeast University, Nanjing, China. His research interests include optical communication networks and network function virtualization.

QING SUN received the M.S. degree from the School of Electronic Science and Engineering, Southeast University, Nanjing, China, in June 2019. He is currently with Huawei Technology Company, Ltd., Nanjing. His research interests include optical communication networks and virtual optical networks.

BIN CHEN received the B.Sc. degree from the School of Electronic Science and Engineering, Nanjing University of Posts and Telecommunications, Nanjing, China, in June 2017. He is currently pursuing the M.S. degree with the School of Electronic Science and Engineering, Southeast University, Nanjing. His research interests include wireless networks and machine learning.

JIAHUA GU received the B.Sc. degree from the School of Electrical Engineering and Automation, Nanjing Normal University, Nanjing, China, in June 2016. He is currently pursuing the Ph.D. degree with the School of Information Science and Engineering, Southeast University, Nanjing. His research interests include C-RAN and machine learning.

• • •